Characteristics of a 16x16 Fine-Pixel Cadmium-Zinc-Telluride Detector

D. P. Sharma*[a], J. A. Gaskin[b], B. D. Ramsey[a], and P. Seller[c]

[a]Marshall Space Flight Center, SD 50, Huntsville, AL 35812, USA
[b]University of Alabama at Huntsville, Huntsville, AL 35899, USA
[c]Rutherford Appleton Laboratory, Chilton, OXON, OX110QX, UK

ABSTRACT

Cadmium-Zinc-Telluride (CdZnTe) multi-pixel detectors are ideal for astrophysical application. As part of ongoing research at the Marshall Space Flight Center (MSFC), we are working to develop a 64x64 fine-pixel detector for use at the focus of high-resolution grazing-incidence optics. As a first step towards achieving this goal, we present results from a 16x16 fine-pixel CdZnTe detector, 2mm thick, having a pixel pitch of 300μm and an inter-pixel gap of 50μm.

Keywords: CdZnTe, pixellated detectors, HERO, X-ray

1. INTRODUCTION

Recent results from the Chandra Observatory are revolutionizing our understanding of the universe at soft X-ray energies. These results were made possible through the use of high-quality grazing-incidence X-ray optics that give a combination of very-high angular resolution (0.5 arcsec) and very-high sensitivity ($4x10^{-15}$ ergs/cm^2/s (0.4-6keV) with an exposure time of 10^4 sec)[1]. Such optics have yet to be used at high energies and thus, the hard X-ray region remains relatively unexplored. To study complex hard X-ray phenomena such as, for example, the fine structure of the galactic center above 20keV; to search for and study cyclotron lines and; to study of spectral changes at higher energies such as high-energy tails in black hole sources, requires a high sensitivity and high spatial resolution at energies above 20keV. To achieve this, MSFC is fabricating moderately-high-resolution (15 arcsec) hard-x-ray grazing incidence optics and suitable detectors to go at the focus of these optics.

Recent developments show that CdZnTe offers great promise as a hard X-ray detector. Due to its relatively high effective atomic number, even a 2mm thick CdZnTe crystal has ~100% absorption efficiency up to 100keV, and its ~ 2eV band gap permits operation at or near room temperature with excellent energy resolution. CdZnTe can also be pixellated through the use of simple contacts, which facilitates fine imaging spectroscopy. Because of these attributes, MSFC has initiated a study of CdZnTe detectors for possible use at the focus of its hard X-ray optics as part of its High Energy Replicated Optics (HERO) balloon program. It is expected that the launch of the fully developed HERO experiment[2], together with other hard X-ray telescopes under development, will usher in a new era in hard X-ray astronomy similar to that initiated by the introduction of X-ray optics at lower energies.

2. DETECTOR

The detector under study is a precursor to the detector that we plan to use with HERO balloon payload, and also has the potential for a space based high energy X-ray astronomy experiment. The complete detector has two components: a pixellated CdZnTe crystal and an Application Specific Integrated Circuit readout chip (ASIC).

* Dharma.P.Sharma@msfc.nasa.gov; phone 1 256 544-9345; fax 1 256 544-7754; Marshall Space Flight Center, SD50, Huntsville, AL 35812

2.1 CdZnTe

The completed CdZnTe detectors were procured through Metorex Inc who managed the testing and bonding to the ASICs. The CdZnTe crystals were supplied by Imarad and eV Products. All of the detectors were subjected to IR imaging to learn about the quality of the crystals. The crystals from Imarad appeared to be more uniform under this inspection, with fewer visible defects, presumably due to the different growth process used. Crystals with a polished surface showed much superior IR transmission images than etched ones, which resulted in rounding of edges, and probably caused pitted or rough surfaces. All of the crystals were tested to measure their leakage current. All were found to have a pixel resistance ranging from 50GΩ to 70GΩ. Some of the crystals initially had a higher leakage current and were annealed to reduced their leakage current to the above range. After IR imaging, all the detectors were sent to eV Products to have platinum metal contacts sputtered on both sides. The cathode side is a solid planar contact whereas the anode side is a 256-pixel pattern designed to be compatible with the ASIC pattern. The pixel pattern is a 16x16 mosaic with pixel size of 250μm square and 50μm inter pixel spacing, thus, resulting in a pixel pitch of 300μm. Surrounding the pixellated area, and separated by a 75μm gap, is a "guard" electrode structure, which is electrically grounded during detector operation.

2.2 ASIC

The ASIC was designed by the Rutherford Appleton Laboratory, England (RAL). The ASIC consists of a Pixel Array Chip (PAC5) and two Shaper-And-Multiplexer-Read-Out-Chip (SHAMROC) integrated circuits. The PAC5 is an array of 16x16 pre-amplifiers, each 300μm x 300μm, and line drivers (Fig. 1)[3]. This chip is gold bump bonded directly to the CdZnTe crystal. The 256 pre-amplifiers on the PAC5 are connected by aluminum wire bonds to two SHAMROCs that shape and amplify the signals then input them to chip comparators. These are then read off the chip by a computer-controlled data acquisition system.

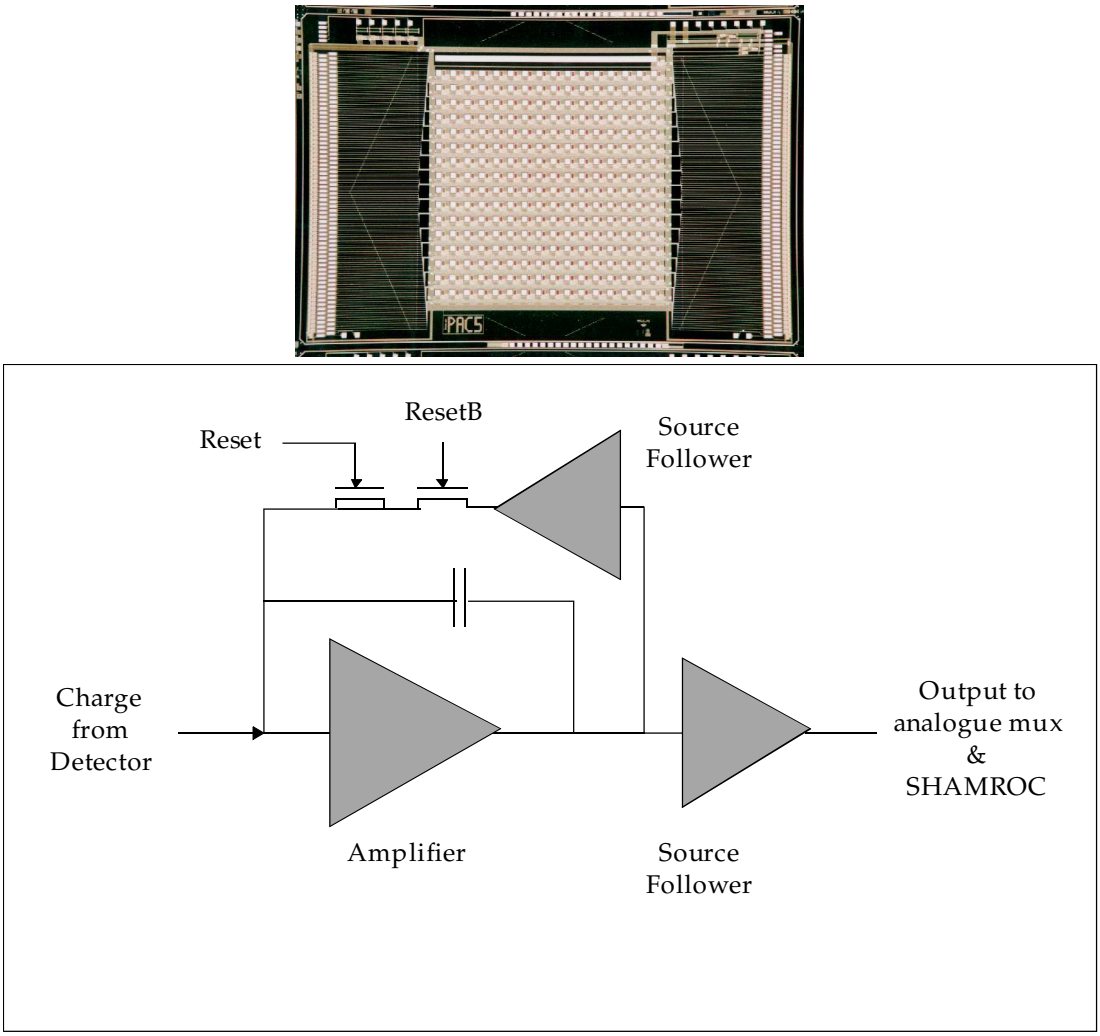

Figure 1: The PAC5 integrated circuit and schematic diagram.

The preamplifiers have a folded cascade stage with optimized input FETs and a feedback capacitance of 100fF to give adequate gain while maintaining gain uniformity between pixels. The noise performance of the preamplifier is designed to give 20e- RMS with a 250fF detector capacitance, 250fF pad capacitance and 10pA leakage when shaped by the 2μs shaper. PAC5 has test inputs via charge injection through dummy reset transistor gates and can be read out on a shift-register-driven multiplexer test output. Both PAC5 and SHAMROC are built on the Mietec 0.7μm CMOS process.

Each SHAMROC contains 128 CR-RC shaper, peak-hold and comparator circuits. A signal above an adjustable threshold in any pixel flags the readout electronics which in turn sends the analogue value and address of the pixel hit to off-chip electronics. This action resets the shaper of this pixel only.

The signal from each PAC5 amplifier is shaped by a CR-RC amplifier in the SHAMROC with a voltage gain of about 40 and fed to a peak-hold circuit. If the signal is above the set threshold it sets a flag in the readout logic and enables the corresponding peak-hold circuit to store the peak value. Only this channel is affected by the signal, enabling the rest of the system to continue to acquire data. This Hold signal also raises a flag, which will trap a readout pointer enabling the analogue multiplexer and routing the stored value from the channel to the analogue output. The channel address and a Data Valid signal are also output to indicate that the data on the output is valid. The readout pointer passes

through the logic for the 128 channels until it emerges at the PtroutB output and is fed around to the next SHAMROC chip, or back to its own PtrinB if standing alone (see figure 2). The pointer logic is designed to allow the pointer to skip channels with no data. A single channel readout cycle takes 1 µs and the readout logic then applies a reset to the peak-hold and comparator circuits of the channel and resets itself. The functional block diagram is depicted in Figure 2. Figure 3 depicts the mounted detector and ASIC. Further details regarding this ASIC can be found in Seller *et al*[3].

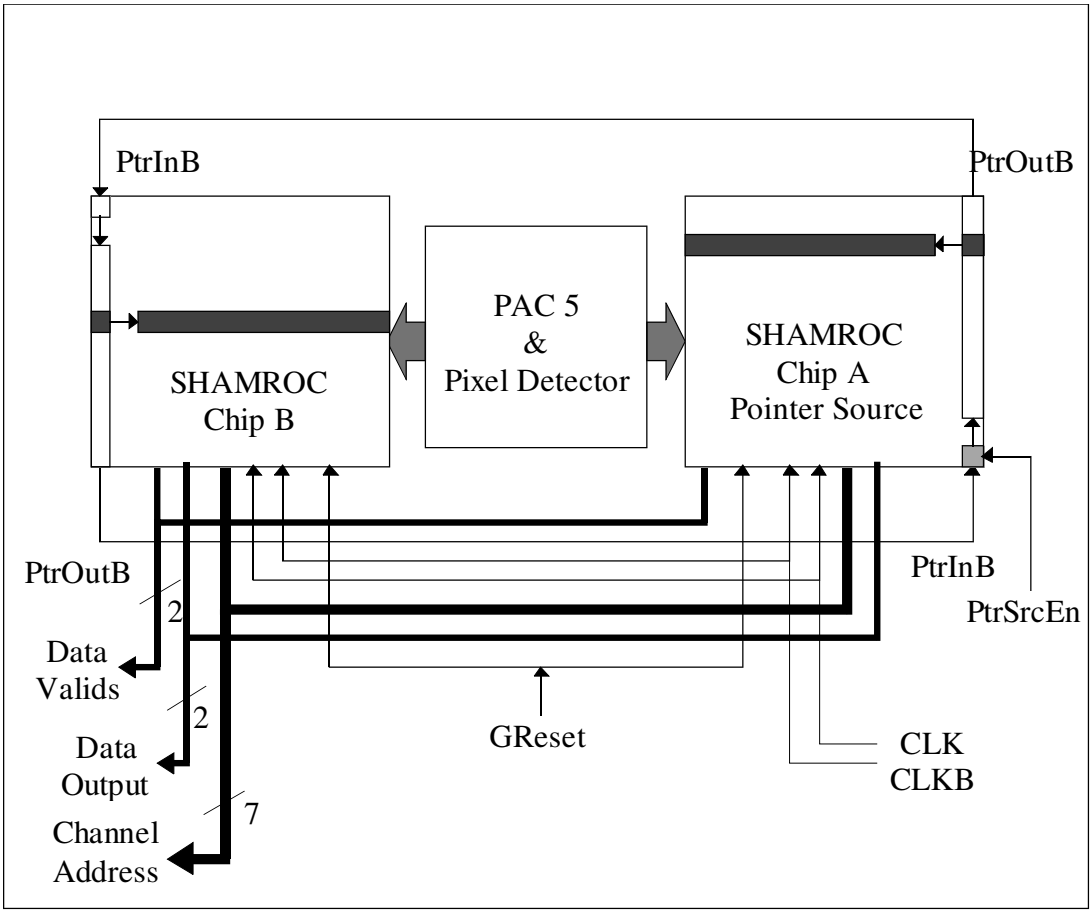

Figure 2: System block diagram.

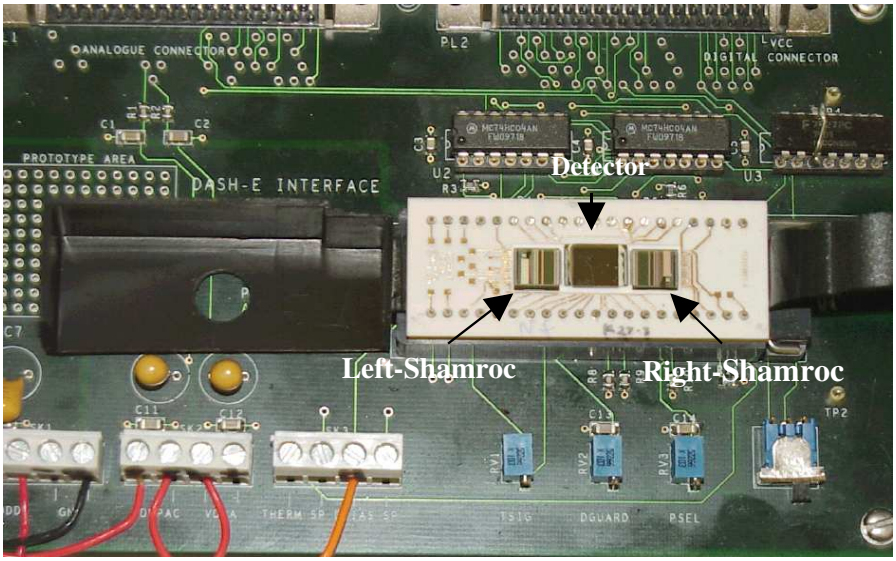

Figure 3: Detector with ASIC mounted on the interface board.

3. EXPERIMENTAL WORK

3.1 Set-Up

The detector was mounted on the interface board shown (Fig. 4) which was cooled via a gaseous nitrogen system to between 0°C and –20°C, and connected to a computer via two National Instruments PCI cards. One of the cards (PCI 6111E) has a 12-bit ADC to process analog signals and a 16-bit DAC to process the digital signals or control digital circuits. The second card (PCI-DIO-32HS) is a 32 bit, parallel, digital I/O interface card and was used to control the ASIC. Detailed testing of the detector was performed through the use of National Instruments' LabView operating software. After collecting data in various operation modes, they were analyzed using FORTRAN and other dedicated programs.

3.2 Methodology

Our experimentation focused on three main areas; the noise performance of the detector and their energy resolution, the linearity of their energy response, and the quantification of charge sharing and charge loss. In order to test the first two areas, the detector was uniformly illuminated with several uncollimated monochromatic sources ranging in energy from 5.9keV (Fe^{55}) to 60.0keV (Am^{241}). Several pixels across the detector were tested and characterized. To study charge sharing and charge loss, data from a block of 9 adjacent pixels (3x3 pixel array) were recorded simultaneously. In this way, charge sharing could be considered between the central pixel of this smaller array and its surrounding pixels.

4. EXPERIMENTAL RESULTS

4.1 Detector noise and resolution

Figure 4 shows a spectrum of Fe^{55} (5.9keV) indicating the noise performance of the detector. We estimate that in the present set-up, the FWHM noise content is around 1.0keV. Because of the functioning of the ASIC, however, the minimum signal threshold level is actually higher than this, at about 2.5keV.

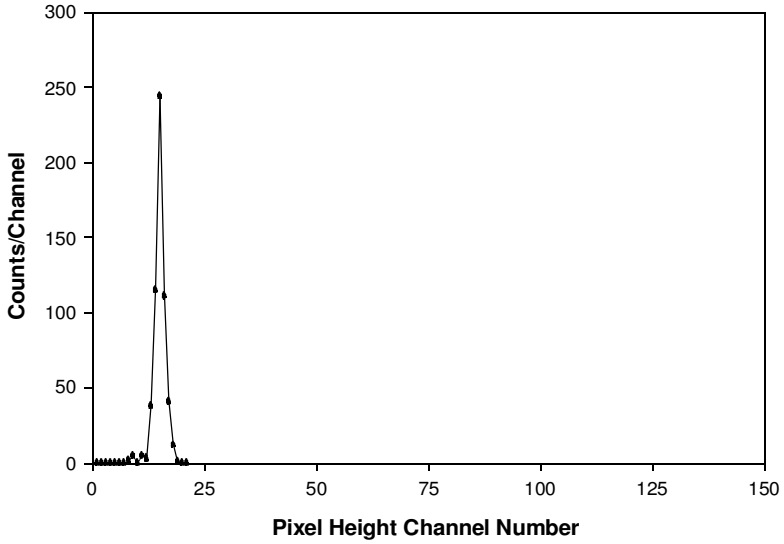

Figure 4: Measured spectrum at 5.9keV for a single pixel when irradiated by an uncollimated source (bias voltage 600v).

Table 1 shows the experimentally measured energy resolution at various energies for unshared events in a 2-mm-thick Imarad detector. These measurements confirm that the energy resolution is dominated by a constant noise component, which results in a linear dependence with energy rather than a 1/sqrt(E) dependence. Similar values are obtained for the reconstructed spectrum after summing the shared signals from various pixels discussed later.

Table 1. Measure values of energy resolution.

Energy (keV)	Resolution (%)
5.9	13.3
17.4	6.1
22.1	3.4
32.1	3.3
44.2	2.8
59.9	2.0

Figure 5 shows the linearity of energy response. As can be seen, a small DC offset is present in the ASIC readout.

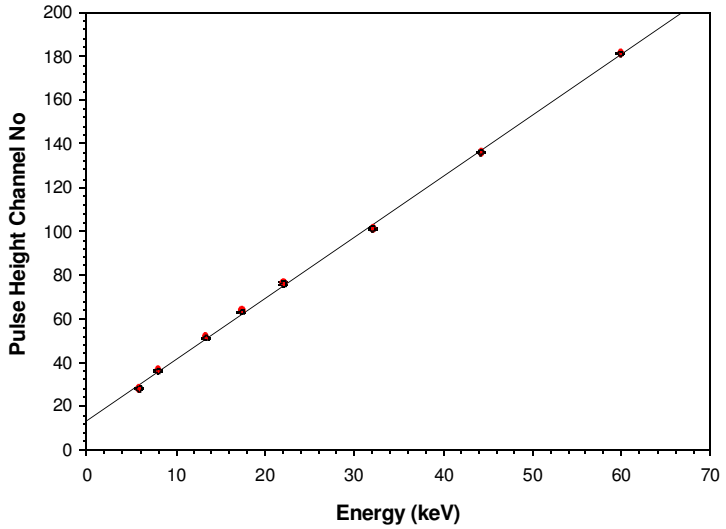

Figure 5: Energy response of the 2mm thick detector.

4.2 Charge Sharing

With such fine pixels, we should expect that a significant number of events will be shared between adjacent pixels[4]. To investigate this, we irradiated the detector with an uncollimated monochromatic source and recorded data simultaneously from a block of 9 pixels. The central pixel of the block can then be used to estimate the shared charge and to generate a reconstructed spectrum. This is achieved by accepting, on the central pixel, only those shared events that are shared with surrounding pixels but have larger signal on the central pixel indicating that the event has originated on it (for incident energy of 60keV). We have divided the shared events in to three groups; those shared between only two pixels "doubles"; those shared among three adjacent pixels "triples" and; those shared among four adjacent pixels "quadruples" (as would happen in the common corner of 4 adjacent pixels). All other events are tagged as unshared. At 60keV, of the 56% of all events measured to be shared, the number of doubles for the middle pixel was observed to be 46% and the rest, 10%, were triple and quadruples.

Data were collected at, 44.5keV and 60.0keV for various detector bias voltages. Figure 6 shows one such observation for a 2mm thick detector with 600v bias voltage. The large peak at the lower energies of the observed raw spectrum is due to shared events mostly from adjacent pixels.

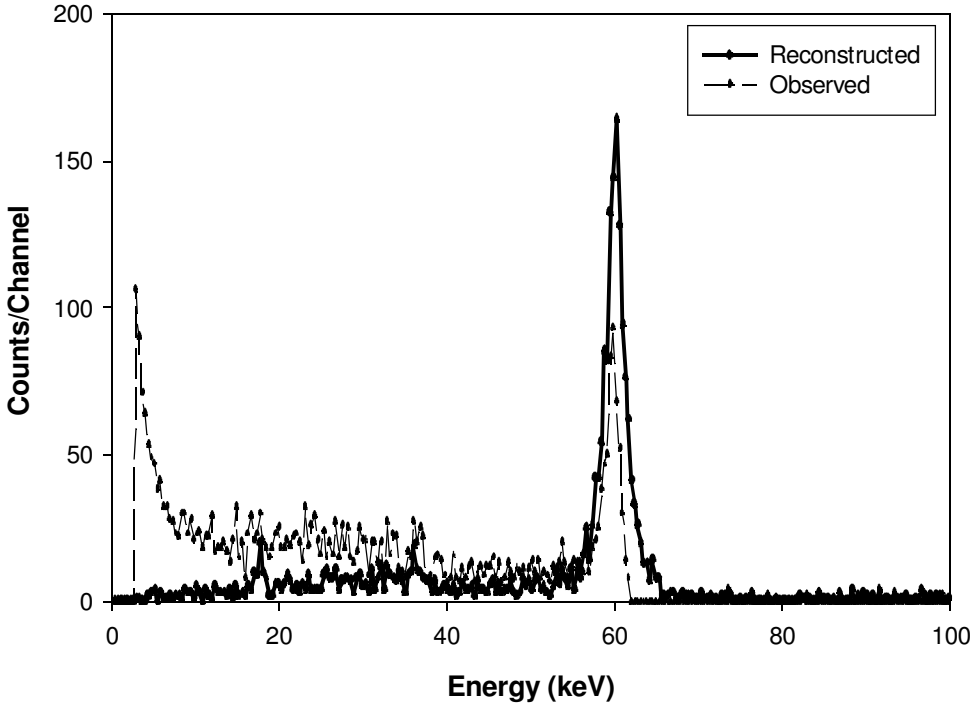

Figure 6: Shows the raw observed spectrum and the reconstructed spectrum (shared events added back into the photopeak) for a single pixel when the detector is illuminated by an uncollimated Am^{241} (60keV) source.

Adding these signals back to their appropriate initial-interaction-site pixel, determined by which pixel has the larger portion of a shared event, cleans the spectrum considerably, as the figure shows. The energy resolution for the reconstructed curve is calculated to be roughly 2.0%. It is interesting to note that there is very little change in position of the peak after the signals are summed indicating little or no charge loss at 60keV for shared events, which necessarily originate in or around the inter-pixel gap.

Figure 7 shows the observed (unreconstructed) spectrum for 44.5keV obtained for the 2mm thick detector at three different detector bias voltages. It can be seen from Figure 7 that as the bias voltage is increased, the charge collection efficiency improves resulting in a larger and more distinct photopeak. The photopeak curve for each bias voltage (from 100v-600v) was plotted and fitted with a Gaussian. Table 2 lists the peak height channel for each voltage. As the bias voltage nears 600v, the change in the peak height channel becomes small.

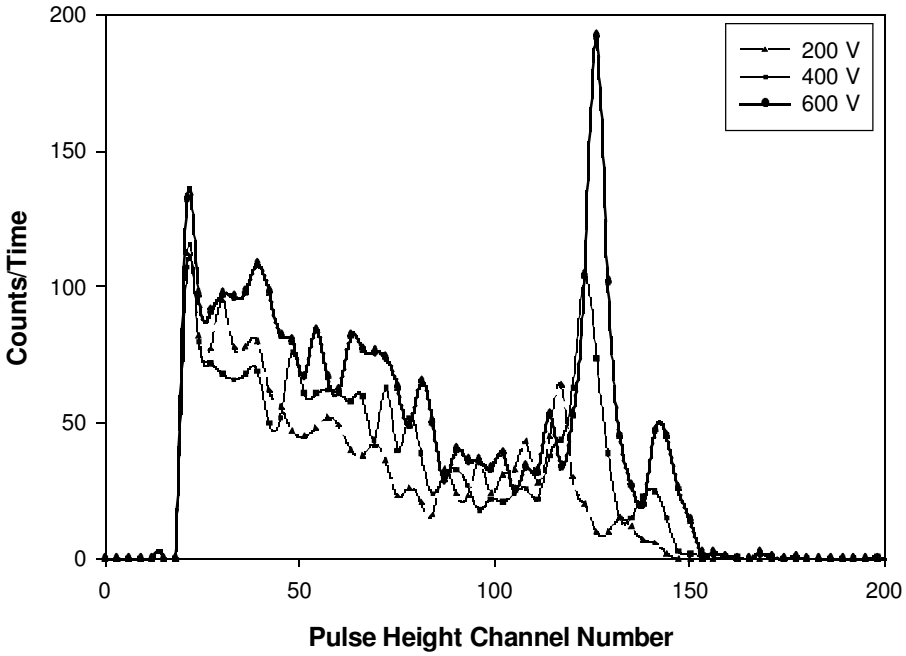

Figure 7: Observed spectrum at 44.5keV at three different detector biases.

Table 2: Photopeak channel number for various detector bias voltages. Data in this table is also represented in Figure 7.

Bias Voltage (v)	Peak Channel Number
100	101
200	112
300	119
400	123
500	124
600	126

5. SIMULATION RESULTS

We are developing a Monte Carlo simulation of the detector response to understand the observed behavior. The simulation configuration is a randomly distributed set of photons uniformly illuminating a 2mm thick detector consisting of 9 pixels (3x3 pixel array). Each pixel is 300μm square, as in our experimental case. The electric field is assumed to be uniform across the detector (with bias voltage of 600v). Each photon, with a given energy, is exponentially attenuated and has a finite probability of interacting with a cadmium, zinc, or tellurium atom. If photoelectric absorption occurs and there is a K-shell interaction, the probability for each characteristic fluorescent photon that can be produced in a K-shell interaction is calculated. Also, a photoelectron is ejected from the atom whose energy is equal to the incident photon energy minus the characteristic photon energy. The re-emitted fluorescent

photon travels some distance (depending on its energy) and can either be reabsorbed, emitting a photoelectron, or ejected from the detector. If there is no K-shell interaction, the full charge cloud is created at the initial photon interaction point in the detector. As the charge cloud drifts towards the collection electrode, it diffuses. The lateral spread of this diffusion can be approximated by a Gaussian with a standard deviation σ. The amount of spread is dependent on the incident X-ray energy, the electric field magnitude, E, the charge carrier mobility, μ, and the detector thickness, *d*. As the amount of spreading increases, so does the chance that a single event will be shared over multiple pixels. The equation below gives the approximation for the lateral charge spread that was used[5].

$$\simeq \sqrt{2\ t\ (\mu kT/e)} = \sqrt{\frac{2\,kTd}{eE}}$$

Where *k* is Boltzmann constant, T is the temperature, and e is electron charge. The final position of each charge carrier in the charge cloud is recorded.

In this way, the amount of charge shared between two or more pixels for each incident photon can be determined. We have utilized this program to calculate the expected spectrum for uniform illumination of a single pixel both with and without reconstructing shared events (Fig. 8). From this spectrum, one can see that in the presence of charge sharing, some of the events that would normally be in the photopeak are now in the lower energy tail. However, the low energy tail also includes events that have originated on surrounding pixels. These events will not contribute to the photopeak after reconstruction. When the spectrum is recreated, the photo peak becomes larger and the escape peaks for cadmium and tellurium can be seen.

The simulation also includes effective charge loss due to a lower limit threshold, which is determined by experimentation. This pixel threshold effectively removes any shared charge that is below the detection threshold (2.5 keV), which is too small to register. However, the simulation does not yet include the charge loss due to field lines terminating in the inter-pixel gaps or to the charge collection efficiency of the detector.

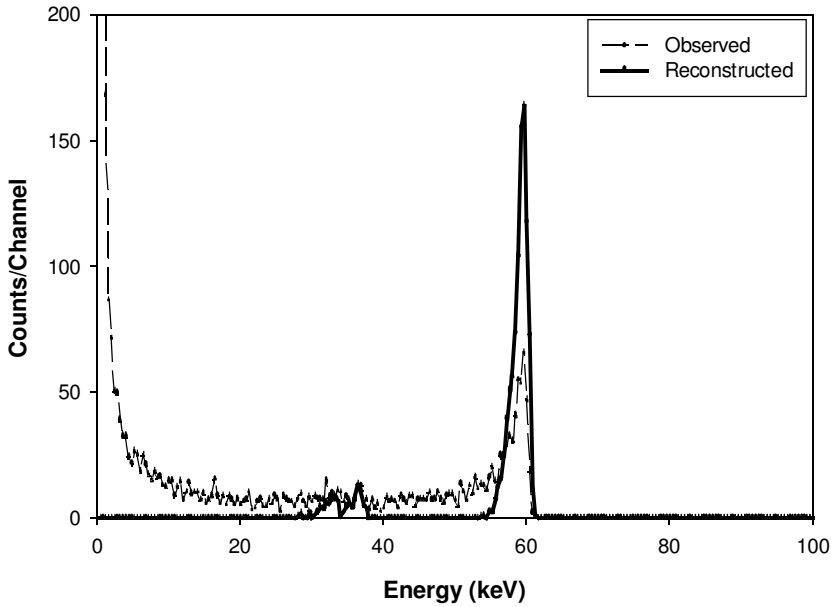

Figure 8: Simulated observed and reconstructed spectrum for Am^{241}. The two smaller peaks are the escape peaks associated with cadmium and tellurium. The bias voltage was set at 600v and the detector thickness was 2mm.

By comparing the simulated results of charge sharing to the experimental results, a diffusion coefficient $\sigma \cong 43\mu m$ was determined to give the best fit. Table 3 compares the simulated to experimental percentages for sharing for incident photons with energies of 22.2keV, 44.5keV, and 60.0keV.

Table 3: Simulated and Experimental charge sharing results for the 2mm thick detector (bias voltage was 600v).

Energy (keV)	% Shared events (Measured)	% Shared events (Simulation)
22.2	30	37
44.5	49	50
60.0	56	55

The Gaussian diffusion standard deviation is dependent on the detector bias voltage. As the voltage decreases, the amount of diffusion increases (increasing the amount of shared charge). Table 4 shows simulated measurements using an incident X-ray energy of 44.5keV and 60.0keV.

As in the experimental results, an event is counted as being shared when charge from a single event is shared between two or more pixels and the majority of charge from that event is detected by the central pixel. For a K-shell interaction between Cd or Te the most probable resulting characteristic photon energies are 23.2keV and 27.5keV respectively[6]. If the incident photon energy is 44.5keV the majority of charge from a single event no longer has to be on the central pixel, but rather can be on the surrounding pixels. This is because the remaining photoelectron energy is equal to the incident photon energy minus the characteristic photon energy. These events are not counted as shared events on the originating pixel, even though they are actually being shared. Therefore, when fluorescence is excluded from the simulation for 44.5keV, the amount of shared charge changes only slightly. When the incident photon energy is 60.0keV and fluorescence is included, despite the dispersion of the characteristic photon, the majority of charge is still on the central pixel and is counted as being shared.

Table 4: Simulation results showing charge sharing for various bias voltages when fluorescence was included and excluded.

Energy (keV)	Bias Voltage (V)	% Of shared events with fluorescence	% Of shared events without fluorescence
44.5	200	60	66
44.5	400	53	56
44.5	600	50	53
60.0	200	69	67
60.0	400	60	59
60.0	600	55	55

6. FUTURE WORK

The next phase of this project will include employing a 10μm pinhole attached to an X-ray source to perform a raster scan across the detector. This will give us a more complete picture of charge sharing and charge loss on a much finer scale and allow us to develop a response matrix of the detector. It will also permit us to investigate the effective spatial resolution of the detector, which through charge sharing, which permits interpolation, can be better than the detector pixel pitch. We will also be able to correlate crystal defects and impurities with the detector response. Results from all these measurements will be compared to the simulations, which we intend to refine by including electric field modeling.

REFERENCES

1. Chandra X-ray Center, Chandra IPI teams. *Chandra Proposer's Observatory Guide*, Cambridge, 2000. http://cxc.harvard.edu.
2. B.D. Ramsey, C.D. Alexander, J.A. Apple, R.A. Austin, C.M. Benson, K.L. Dietz, R.F. Elsner, D.E. Engelhaupt, J.J. Kolodziejczak, S.L. T. O'Dell, C.O. Speegle, D.A. Swartz, M.C. Weiskopf, and G. Zirnstein, "HERO: High-Energy Replicated Optics for a Hard-X-Ray Balloon Payload"™, SPIE 4138, 147, 2000.
3. P. Seller, W. J.F. Gannon, A. Holland, G. Iles, B. Lowe, M. L. Prydderch, S. L. Thomas, R. Wade, "Silicon pixel detector for X-ray spectroscopy", SPIE 3445, 584, 1998.
4. D.P. Sharma, B.D. Ramsey, P. Seller, T. Tumer, "A Study Of Charge Sharing in Pixellated Cadmium-Zinc-Telluride Detectors",™ IEEE 12th International Workshop, San Diego, CA, 2001.

5. G. Knoll, *Radiation Detection and Measurement*, Third Edition, John Wiley and Sons, Inc., New York, 1999.
6. E. Browne, R. B. Firestone, *Table of Radioactive Isotopes*, John Wiley and Sons, Inc., New York, 1986.